

SUBSYNCHRONOUS VIBRATIONS IN A HIGH PRESSURE

CENTRIFUGAL COMPRESSOR: A CASE HISTORY

B. F. Evans and A. J. Smalley
Southwest Research Institute
San Antonio, Texas 78284

This paper documents two distinct aerodynamically excited vibrations in a high pressure low flow centrifugal compressor. A measured vibration near 21 percent of running speed was identified as a non-resonant forced vibration resulting from rotating stall in the diffuser; a measured vibration near 50 percent of running speed was identified as a self-excited vibration sustained by cross-coupling forces acting at the compressor wheels. Measured data shows the dependence of these characteristics on speed, discharge pressure, and changes in bearing design. Analytical results are presented which provide strong evidence for the exciting mechanisms of diffuser stall and aerodynamic cross-coupling. Additional results show how the rotor characteristics would be expected to change as a result of proposed modifications. The satisfactory operation of the compressor after these modifications is described.

INTRODUCTION

Two distinct subsynchronous vibrations were encountered in commissioning an eight stage centrifugal compressor. The 3170 kW (4250 hp) compressor was specified to meet API 617 standards and is designed to run at 13,500 rpm with a design discharge pressure of 180 bar (2600 psi) and flow of 33,800 m³/h (21,000 SCFM).

The compressor (Figure 1) is mounted in 5-shoe tilting-pad bearings with load on pad (5SLOP) and length to diameter ratio, L/D, of 1. Oil breakdown seals of the balanced floating type were initially located inboard of the bearings. Total rotor length is 1810 mm (71.3 inches) with a total mass of 245 Kg (total weight of 540 lb), and a bearing span of 1360 mm (53.7 inches).

Manufacturer's test stand data, from a run in a vacuum, showed a reasonably well damped first critical at about 5700 rpm, but there was a slight indication of subsynchronous response at the first critical frequency when the compressor was taken to overspeed (14,500 rpm).

After installation, the compressor ran satisfactorily on recycle up to the limiting horsepower capability of the gas turbine drive under recycle conditions--12,400 rpm. Closing the recycle valve would start to build discharge pressure, but at about 96.5 bar (1400 psi) a disturbing vibration started with a frequency of about 6000 cpm. This vibration would grow and decay but its maximum excursion would increase rapidly to above 50 μ m (2 mils) as the recycle valve was further closed.

An initial change was made by cutting the bearing effective length by close to 50 percent without any change to clearance or preload. Because the bearing is lightly loaded, this change would tend to reduce stiffness, causing more amplitude and therefore more dissipation of vibration energy at the bearings. This change reduced the frequency of the unstable vibration to about 5700 cpm for a discharge

pressure of 121 bar (1750 psi). Before the unstable vibration peak amplitude became intolerable, maximum vibration amplitude at 5700 cpm and 121 bar was about 20 μm (0.8 mils), peak-to-peak. As discharge pressure was increased above 121 bar the unstable vibration amplitude increased exponentially. This modification allowed limited operation which had been impossible without the bearing change.

Along with improved control of the unstable vibration a new vibration at 21 percent of running speed with amplitudes of about 25 μm (1 mil) was observed. Thus, the bearing change allowed temporary operation but clearly showed that there were two subsynchronous vibration problems to be identified and corrected.

In response to this situation the manufacturer developed more substantial changes to the rotating and stationary elements of the compressor. This paper presents selected results from an independent study involving both measurement and analysis to identify the problems and to evaluate the proposed modifications to the rotor and its suspension. The objective of the paper is to contribute to the available body of data on subsynchronous vibration of turbomachinery and to show how existing state of the art criteria and analyses can be effectively applied in design and troubleshooting.

MEASURED DATA

The data presented was obtained using four installed 45° proximity probes. The two bearing locations are identified as drive end (DEX, DEY), and non-drive end (NDEX, NDEY).

Conditions are referred to as "original bearings" and "MOD 1 bearings;" the original bearings were 89 mm (3.5 inches) in diameter and 92 mm (3.625 inches) in total length with a groove 3.2 mm (0.125 inch) wide running circumferentially through the middle of each pad, creating two lands each 44.4 mm (1.75 inches) wide. The MOD 1 bearings were made from the original bearings by cutting the width of each land to 20.7 mm (0.813 inches). For both bearings the machined radial clearance, CP, was 117 μm (4.6 mils) (nominal) and the measured assembled clearance, CB, was 80 μm (3.13 mils) (average) giving a preload, m, of about 0.3.

Figure 2 shows the vibration spectrum at non-drive end with original bearings at 11,100 rpm and a discharge pressure of 117 bar (1700 psi); the 6000 cpm vibration is pronounced with an amplitude of 23 μm (0.9 mils). Running speed vibration amplitude is approximately 13 μm (0.5 mils).

Figure 3 shows vibration spectra at non-drive end for discharge pressures of 121 and 128 bar (1760 and 1850 psi) with the MOD 1 bearings. Speed is again 11,100 rpm. Note that the unstable vibration frequency dropped to 5700 cpm and is again pronounced, but there is now a vibration at 21 percent of running speed whose amplitude is comparable to the 5700 cpm vibration.

In Figure 4 the data has been organized to show how the unstable vibration varies as a function of discharge pressure for the original bearings. The 6000 cpm vibration shows an onset at 96.5 bar (1400 psi) and rapid growth with increasing pressure.

Figure 5 presents similar plots as a function of discharge pressure for the rotor with MOD 1 bearings installed. The 5700 cpm vibration appears at a similar pressure as did the 6000 cpm vibration for the original bearings, but grows more

gradually. The 21 percent vibration first appears noticeable at 96.5 bar (1400 psi) but is limited to about 25 μm (1 mil) as discharge pressure increases. Note also that the drive end amplitudes for the 21 percent (2323 cpm) vibration are much smaller than those at the non-drive end and that the non-drive end amplitudes do not show much variation with pressure. It was observed that the 21 percent vibration tracked running speed at a constant ratio and thus was referred to as such in some of the figures.

ANALYSIS

Subsynchronous vibrations can result from two distinct aerodynamic phenomena: in one the flow disturbances and resultant dynamic forces are directly influenced by the amplitude of mechanical vibration; in the other the flow disturbances and forces are a function of the flow itself and are not significantly influenced by the level of mechanical vibration. The latter are called rotating stall or surge; the former are referred to as self-excited vibrations, and the forces are commonly referred to as Alford forces (ref. 1).

Self-excited vibrations which are sustained by rotor motion generally occur on the order of 50 percent of operating speed. Excitations due to rotating stall fall into two categories which are distinguished by frequency. Impeller rotating stall is characterized by frequencies of approximately 70 percent of operating speed, while vibrations due to diffuser rotating stall generally occur in the 10 percent to 20 percent of operating speed range (ref. 2).

As mentioned above, two subsynchronous vibration problems existed. One subsynchronous vibration was at approximately half speed while the other was at approximately 21 percent of running speed and appeared to track speed. The calculations performed during this project indicated the first problem of half speed subsynchronous vibration was due to a rotor dynamic instability excited by aerodynamic cross-coupling forces. The second problem was believed to be a diffuser stall due to a very shallow flow angle from the wheel into the vaneless parallel wall diffuser.

The following analysis will deal first with the vibration at 50 percent of operating speed, and then vibrations at 21 percent.

Stability Analysis for Original Rotor

A mass-elastic model of the rotor was prepared and a critical speed map was generated as shown in Figure 6. Superimposed are plots of total impedance, Z , as a function of speed for the MOD 1 bearing (impedance = $\sqrt{K^2 + (\omega B)^2}$) where K and B refer to direct bearing stiffness and damping coefficients and ω is rotational speed. There are intersections between bearing lines and the first two rotor critical speed lines at:

- | | | | |
|---|-----------|---|------------|
| ° | 2,800 rpm | ° | 7,300 rpm |
| ° | 4,800 rpm | ° | 11,000 rpm |

The intersections at 2800 rpm and 7300 rpm are in the rigid body regime for first and second criticals and can be expected to be very highly damped. This is confirmed by unbalance response analysis as typified by Figure 7 which shows drive end bearing response as a function of speed for unbalance excitation at shaft center. Based on Figure 7, critical speeds occur only near the 6000 rpm and

10,800 rpm speeds. It was necessary to include stiffening effects of labyrinth and ring seals to match measured data.

The stability of the unit was calculated for the first forward mode and the results are presented in Figure 8. This plot illustrates the detrimental effect on stability of increasing aerodynamic cross-coupling. The estimated aerodynamic cross-coupling load was approximately 1230 N/mm/wheel (7000 lbs/in/wheel) for this compressor under design operating conditions (ref. 4). Based upon experience, a screening criteria was used, for this particular case, of 0.5 logarithmic decrement at low aerodynamic cross-coupling conditions and a 0.2 log decrement at design conditions with full aerodynamic cross-coupling. These criteria proved unattainable for a range of parameter variations and bearing changes evaluated for the existing rotor geometry. The calculated stability for the compressor's first damped natural frequency was marginal at low aerodynamic cross-coupling values and the log decrement tended to zero or below as design operating conditions were approached.

Figures 9 through 12 are a series of bar graphs which review stability comparisons for the original rotor. Two aero cross-coupling values 175 and 1230 N/mm/wheel (1000 and 7000 lbs/in/wheel) are illustrated. Also, shown in the figures is the desired log dec for reference purposes.

Figure 9 illustrates the difference due to original and modified bearings. The MOD 1 bearing shows a slight increase in log dec; however, calculations predict instability at design conditions which is consistent with the measured field data.

Calculations using synchronous bearing coefficients are compared to those with nonsynchronous bearing coefficients for a frequency ratio of 0.5 in Figure 10. Predicted system stability is altered greatly by the use of nonsynchronous bearing coefficients; at design operating conditions the calculated log dec drops from +0.1 to -0.25. In view of this significant difference, all other predictions account for frequency dependence of the tilting pad bearing characteristics.

The effect of preload on the MOD 1 bearing is shown in Figure 11. Increasing preload decreases stability slightly.

Figure 12 summarizes five other bearing modifications considered for this unit. These were:

(1) MOD 1	L/D = 0.5	With Groove	5SLOP	m = 0.3
(2) MOD 2	L/D = 0.5	Without Groove	5SLOP	m = 0.3
(3) MOD 2A	L/D = 0.25	Without Groove	5SLOP	m = 0.3
(4) MOD 3	L/D = 0.5	With Groove	5SLBP	m = 0.3
(5) MOD 4	L/D = 0.5	With Groove	5SLOP	m = 0.0

None of the considered modifications increased the stability significantly above the MOD 1 bearing being used at the time this analysis was performed.

Other portions of the stability analysis addressed the following topics:

- | | |
|------------------------|--------------------------------|
| (1) Hysteretic Damping | (4) Combination of (2) and (3) |
| (2) Seal Ring Lockup | (5) Squeeze Film Dampers |
| (3) Labyrinth Effects | |

While these were not felt to be major factors contributing to the existing sta-

bility problems, some brief comments are worth including. Inclusion of hysteretic damping reduced calculated log dec values. Seal ring lockup, should it occur, significantly increased cross-coupled stiffness values at the seals which adversely affected stability; however, the pressure balancing features of the breakdown seals should preclude lockup. Analysis of the labyrinth seal at the balance drum can indicate either a positive or negative stiffness based upon geometry and certain assumptions (ref. 6). For this rotor, the main effect of ring and labyrinth seals was to act as a soft bearing, thus raising the lateral critical speed above rigid bearing calculations. Squeeze film dampers were investigated. The results were not promising and physical constraints prevented their addition.

Subsynchronous Response Analysis

Rotor system response to forced vibration at a subsynchronous frequency was investigated. This nonsynchronous excitation was imposed upon the shaft under conditions similar to those existing in the field.

The field measured vibrations in the vicinity of 2400 cpm with the MOD 1 bearings did not appear to be a resonant response of the rotor system, but rather the non-resonant response to a large rotating force. Figure 13 shows the predicted rotor response to forced excitation at 21 percent of operating speed. In the vicinity of the measured field vibrations, no resonant response is apparent. For these predictions the excitation force was varied with the square of speed and the magnitude of the force was adjusted to give response levels close to those observed as shown in Figure 13. This required a force of about 580 N (130 lbs) at an excitation frequency of 2400 cpm.

The location of the subsynchronous excitation along the length of the shaft was investigated and the results are shown in Figure 14. It can be seen that as the excitation location is moved toward the discharge end of the shaft, the ratio of amplitudes between non-drive end and drive end approaches that obtained from field data. This gives an indication that the forcing function is being applied near the discharge end of the rotor. The observed difference in measured amplitudes at the two ends is consistent with non-resonant response since at frequencies near resonance both ends are predicted to respond with similar amplitudes wherever the excitation is applied.

Figure 15 shows the effect of the same excitation on rotor response for the original bearing in the machine. The lower predicted amplitudes from the response curve could be attributed to stiffer bearings due to the longer length of the original bearings. This lower amplitude agrees with field data.

Figure 16 illustrates the effect of bearing modifications on the response amplitude in the vicinity of 2400 cpm. The old bearing refers to the original bearing in the machine, while the new bearing refers to the MOD 1 bearing operational at the time of this analysis. The minimum response amplitude was achieved with the old bearing which was an unacceptable alternative based upon the analysis of vibrations at 5700 cpm. The most beneficial alternatives were those that increased the bearing stiffness and thereby the impedance between excitation point and ground. However, bearing changes alone do not appear to eliminate the problem.

Since the vibrations in the vicinity of 2400 cpm appeared to track speed, were not related to a resonant rotor condition, and were at a frequency of approximately 21 percent of operating speed, an investigation was begun to determine if they could be attributed to rotating stall in the diffuser. Published data

concerning stall frequency ratio versus inlet flow angle is shown in Figure 17 for comparison with the observed vibration frequency. It is seen that diffuser rotating stall can occur in the 10 to 20 percent of operating speed range (ref. 2).

The angle at which flow enters the diffuser affects whether or not a stall condition might occur in a diffuser. Published criteria from two sources (refs. 2 and 3) for the critical inlet flow angle versus diffuser width to inlet radius ratio are shown in Figure 18. Based upon system geometry, the predicted flow angle at design conditions lies close to the criteria line. Flow angles below the curve shown in the figure predict rotating stall in the diffuser while angles above indicate diffuser stall should not occur. The width to radius ratio for the last stage of the subject machine was originally 0.029. Included in Figure 18 are predicted flow angles for a revised system which has a diffuser width to radius ratio of 0.021, and these will be discussed in more detail later in this paper.

Analysis of Revised Rotor Design

Since neither of the two subsynchronous vibrations appeared to be controlled at the same time by bearing changes alone, major shaft modifications were considered. The basis for the redesign of the shaft was that a stiffer shaft with a shorter bearing span and larger diameter shaft at the bearings should increase the first critical speed and thus alleviate the half speed vibration problem. At the same time the impedance between rotating stall excitation and ground would be increased, so reducing sensitivity to this excitation. To achieve this, the shaft was modified in the area outside of the balance drum and wheels; the diameter was increased at the bearings, the seals were moved outside the bearings (so that the bearings operate in a high pressure region) and both seal and bearing were redesigned. This also necessitated a change to the spacer in the drive coupling.

Total rotor length is 1700 mm (66.82 inches) and total rotor weight is 2450 N (550 lb). Bearing span was decreased by 186 mm (7.31 inches) to 1180 mm (46.4 inches). Diameter of the shaft at the bearings was increased to 102 mm (4 inches) with an L/D of approximately 1/2. No circumferential groove was included and a 0.2 nominal preload was called for. The seals were of a three lobe type and were located just outside of the bearings.

These modifications to the rotor required a new shaft to be built; however, to save as much time as possible, the area of the shaft which held the wheels and the labyrinth were not altered so that these parts could be reused. Also, the area of the shaft thrust collar was not significantly altered. A new bundle was to be supplied to facilitate the change of the rotor; modifications to the bundle included reductions in diffuser width for all stages and holes drilled in the last stage/labyrinth area to increase last stage flow.

For the revised rotor a critical speed map is shown in Figure 19. Note the higher rigid bearing first critical speed and the stiffer bearing characteristics. There are intersections of the first and second critical speed lines and the bearing total impedance lines at:

- | | | | |
|---|-----------|---|------------|
| ° | 5,500 rpm | ° | 16,000 rpm |
| ° | 6,000 rpm | ° | 16,000 rpm |

In the vicinity of the first critical speed intersection at approximately 70 to 88

kN/mm (4 to 5 x 10⁵ lb/in) support stiffness, the corresponding undamped vibration mode shape shows more deflection at the bearings than the original rotor. This allows the bearing damping to be more effective in dissipating shaft vibrational energy.

Figure 20 shows calculated unbalance response for the drive end bearing as a function of speed for nominal 720 g-mm (1 oz-in) unbalance excitation at shaft center. The predicted first critical speed is now approximately 8200 rpm as opposed to 6000 rpm for the original rotor. As mentioned above, the bearings are in a different part of the vibration mode shape due to the shorter span. The labyrinth has not changed and should still contribute some stiffening effect, but the seals are now outboard of the bearings in an area less sensitive to their dynamic effects (if any).

Rotor stability is summarized in Figure 21 and Table 1 for the revised rotor. The general trend of decreasing log dec with increasing aerodynamic cross-coupling remains; however, the value with zero aero cross-coupling is over 0.7 and the cross-over point for zero log dec has been significantly shifted to the right. Also, the first forward mode's damped frequency predicted under design conditions has increased to above 6000 cpm. It should be pointed out that, for this rotor, a decrease in diffuser widths from the original system causes an increase in the predicted aerodynamic cross-coupling at design conditions. This increase to approximately 1750 N/mm/wheel (10,000 lbs/in/wheel) yields a calculated log dec of approximately 0.2 at design conditions. The increase in the damped natural frequency of the first forward mode is significant and coupled with the increased predicted log dec, the system appears satisfactory from the 50 percent speed self-excited vibration standpoint.

Hysteretic damping, seal and labyrinth effects on calculated stability were investigated. In essence, seal and labyrinth effects did not detrimentally alter the calculated log dec for the system. This was attributed to the fact that the seals were now outboard of the bearings which located them at a different part of the mode shape for vibration at this frequency. Also, the increase in frequency of the first damped critical speed helps increase the margin of stability for all cases investigated.

As with the original rotor the influence of accounting for nonsynchronous tilting pad coefficients was significant.

The predicted flow angles and their relationship to the predicted diffuser stall margin for the modified rotor and diffuser were previously included as part of Figure 18. The changes achieved a distinct increase in margin by over 2° relative to the original design. Coupled with the stiffer shaft, which reduced sensitivity to this excitation by a factor greater than 2, the new design was expected to see a substantial reduction if not total elimination of the 21 percent speed vibration.

The narrower diffuser passages increased the predicted aerodynamic cross-coupling as mentioned previously. The trade-off of higher aero loadings on the wheels versus eliminating diffuser stall is self-evident.

Running Experience with Revised Rotor

The rotor modifications described above have been installed. The compressor has been run to near design discharge pressure and speed with negligible self-

excited vibration. There is a slight hint of vibration at about 20 percent of running speed, but the levels are quite tolerable.

COMPARISON WITH AN ALTERNATIVE STABILITY CRITERIA

A comparison of past unstable compressors with a suggested stability screening criteria was recently presented (see Reference 7). Figure 22 is reproduced from this reference and plots the product of discharge pressure and pressure rise against the ratio of operating speed to first rigid bearing critical speed. The diagonal band is the suggested criteria of Reference 7, with rotors to the left of the leftmost line considered satisfactory.

To evaluate the applicability of the criterion to the compressor under consideration in this study, three points have been superimposed on Figure 22:

- (1) The original design point.
- (2) The design point with the revised rotor.
- (3) The point at which vibration levels become intolerable with the MOD 1 bearing.

All these points lie to the left of the criteria band, indicating that this particular compressor requires a more conservative stability criterion than that of Reference 7.

The potential benefits of such a screening criterion as that proposed in Reference 7 are substantial. However, it appears that a more extensive data base is needed with some adjustment of the criterion band before universal application is contemplated.

CONCLUSIONS

1. This study adds to the data base of published information on subsynchronous vibration of centrifugal compressors.
2. The observed vibration near 50 percent of running speed appears to be a self-excited vibration due to self-sustaining aerodynamic cross-coupling effects.
3. Prediction of log decrement using published empirical data for aerodynamic cross-coupling (ref. 4) and nonsynchronous tilting pad bearing coefficients indicates that the rotor would have a damped critical speed with negative log decrement and frequency near (but below) that observed under design conditions; with zero aero cross-coupling the predicted log decrement is 0.35.
4. Using the same analysis for a design with revised rotor, bearings and seals, log decrement with full aero cross-coupling was predicted to be 0.2 and with zero aero cross-coupling to be 0.7.
5. With this redesigned rotor, subsynchronous vibrations were negligible.
6. There is strong evidence that vibration observed at about 21 percent of running speed was a non-resonant vibration excited by diffuser rotating stall.
7. Observations suggest that operation near to the diffuser rotating stall criteria of References 2 or 3 can result in this form of aerodynamic excitation.

8. If there is insufficient impedance between excitation point and ground, significant vibrations near 20 percent of running speed can result from diffuser rotating stall excitation.

REFERENCES

1. Alford, J. S., "Protecting Turbomachinery from Self-Excited Rotor Whirl", J. Eng. Power, Vol. 87A, 1965, pp. 333-344.
2. Frigne, P., Van Den Braembussche, R., "Comparative Study of Subsynchronous Rotating Flow Patterns in Centrifugal Compressors with Vaneless Diffusers", NASA Conference Publication 2250, Rotor Dynamic Instability Problems in High-Performance Turbomachinery-1982, Proceedings of a workshop at Texas A&M University, College Station, Texas, May 10-12, 1982, pp. 365-381.
3. Senoo, Y., Kinoshita, Y., "Influence of Inlet Flow Conditions and Geometries of Centrifugal Vaneless Diffusers on Critical Flow Angles for Reverse Flow", Journal of Fluids Engineering, March 1977, pp. 98-103.
4. Wachel, J. C., von Nimitz, W. W., "Ensuring the Reliability of Offshore Gas Compressor Systems", Society of Petroleum Engineering of AIME, Journal of Petroleum Technology, November 1981, pp. 2252-2260.
5. Benckert, H., Wachter, J., "Flow Induced Spring Coefficients of Labyrinth Seals for Application in Rotor Dynamics", NASA Conference Publication 2133, Rotordynamic Instability Problems in High-Performance Turbomachinery, Proceedings of a workshop held at Texas A&M University, College Station, Texas, May 12-14, 1980, pp. 189-212.
6. Wright, D. V., "Labyrinth Seal Forces on a Whirling Rotor", NASA Contractor Report 168016, January 1983, p. 32.
7. Kirk, R. G., Donald, G. H., "Design Criteria for Improved Stability of Centrifugal Compressors", ASME Publication "Rotor Dynamic Instability", AMD-Vol. 55, pp. 59-71.
8. American Petroleum Institute, "Centrifugal Compressors for General Refinery Service", API Standard 617, Fourth Edition, 1979.

TABLE 1
COMPARISON OF ROTORS

Rotor Model	Critical Speed Map Results, cpm	Unbalance Response Results, cpm	Stability Analysis Results, Frequency/Log Dec cpm
Original	1	4,800	4260/-0.24
	2	11,000	
	3	15,000	
Revised	1	6,000	6110/+0.2
	2	16,000	
	3	20,000	

* Due to narrower diffuser passages, predicted aero cross-coupling forces at design conditions are greater for the revised rotor.

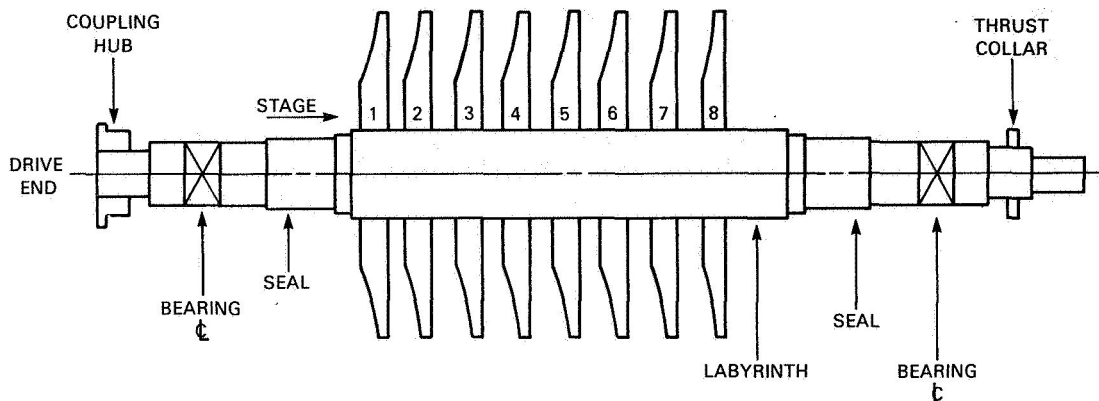


Figure 1. - Rotor sketch of high pressure, low flow centrifugal compressor.

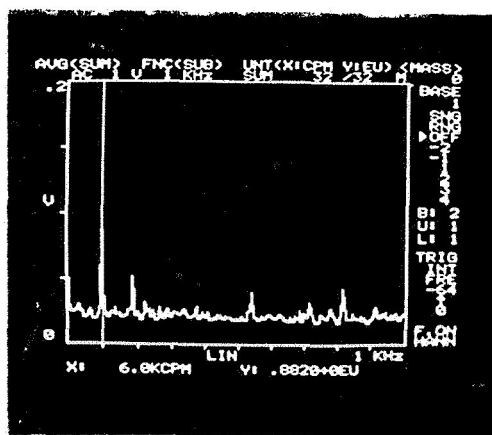


Figure 2. - Vibration spectrum for original rotor in original bearings. Speed, 11 100 rpm; discharge pressure, 1700 psi; non-drive-end X vibration (NDEX).

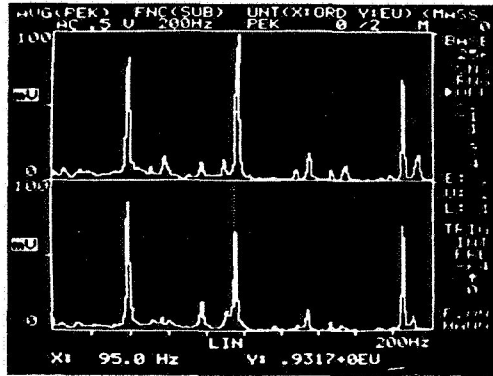


Figure 3. - Vibration spectrum for original rotor in mod 1 bearings. Speed, 11 100 rpm; discharge pressures, 1760 and 1850 psi; non-drive end X vibration (NDEX).

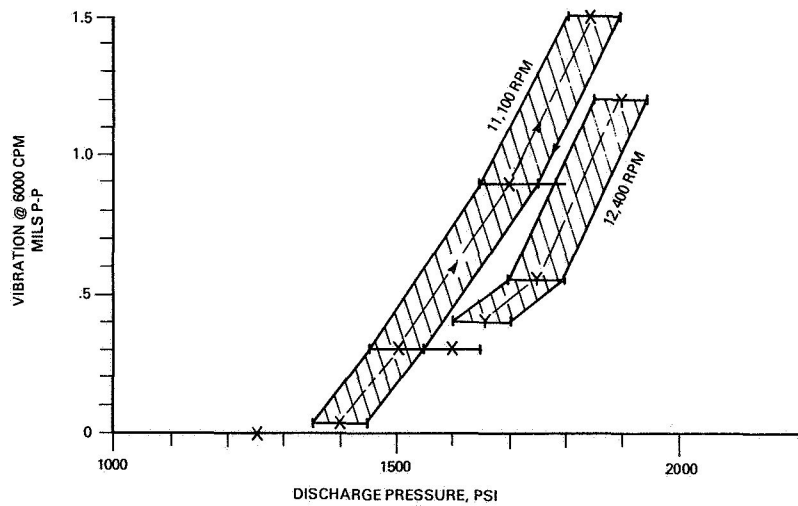


Figure 4. - Vibration as a function of discharge pressure for original rotor in original bearings.

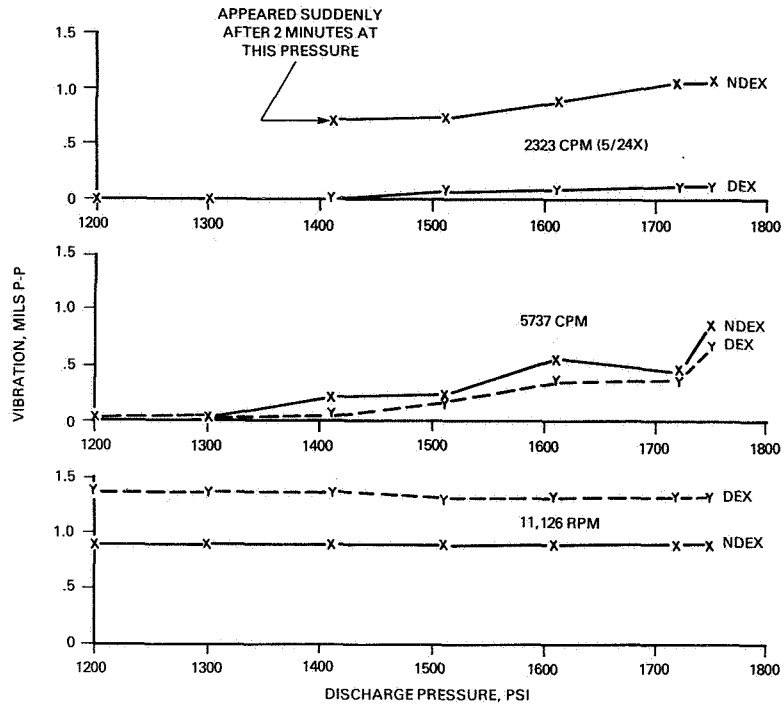


Figure 5. - Vibration as a function of discharge pressure for original rotor in mod 1 bearings. Vibration components at synchronous frequency, half speed, and 21 percent speed; drive-end and non-drive-end X vibration.

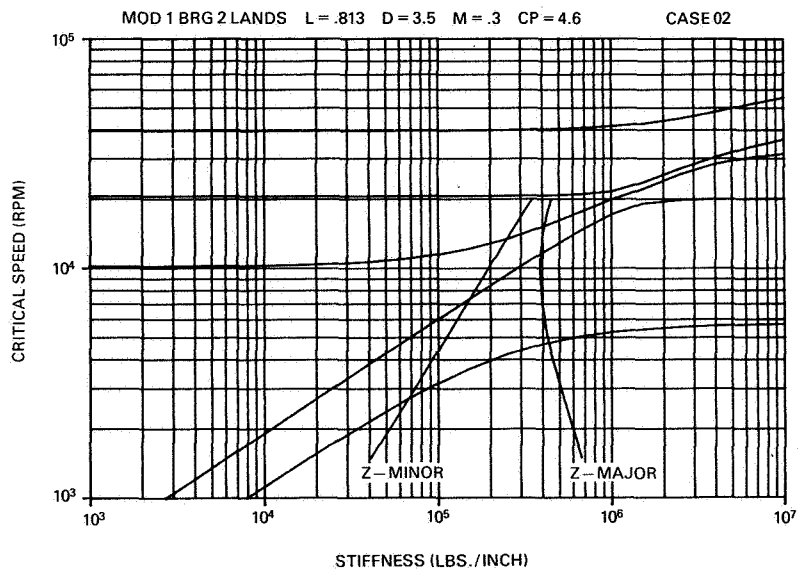


Figure 6. - Critical speed map for original rotor in mod 1 bearings.

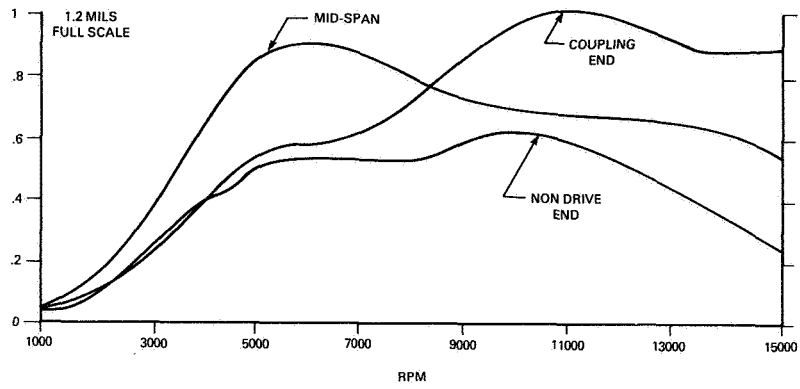


Figure 7. - Unbalanced response for original rotor in mod 1 bearings with 1 in-oz at midspan.

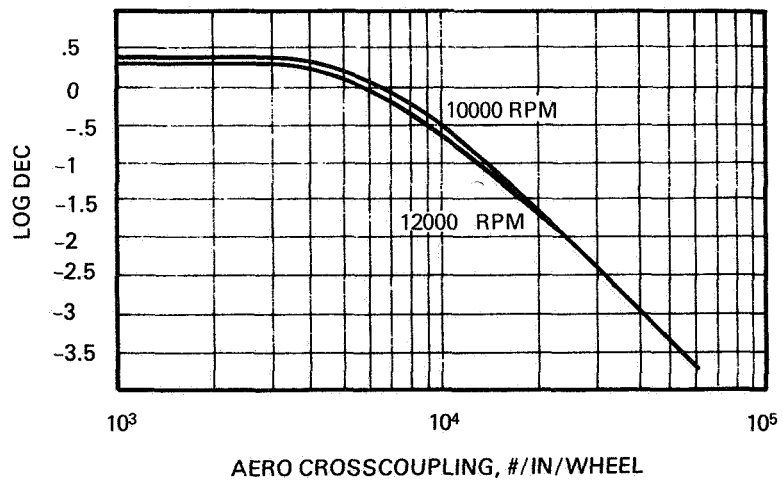


Figure 8. - Rotor stability analysis for original rotor in mod 1 bearings - log decrement as a function of aerodynamic cross-coupling.

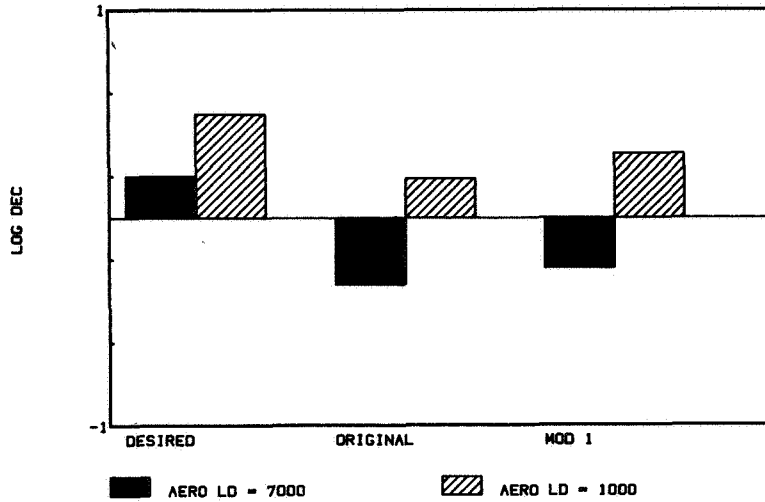


Figure 9. - Stability comparison of original rotor in original bearings versus original rotor in mod 1 bearings. Speed, 12 000 rpm.

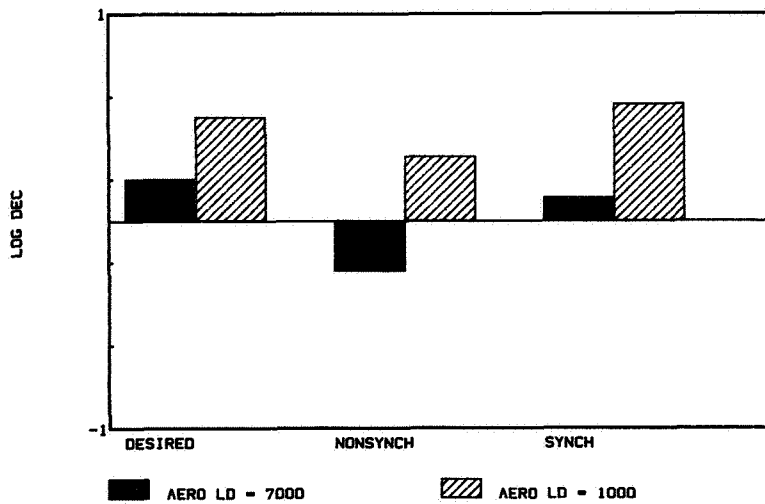


Figure 10. - Comparison of log decrement predicted using synchronous bearing coefficients versus log decrement predicted using nonsynchronous bearing coefficients - original rotor in mod 1 bearings. Speed, 12 000 rpm.

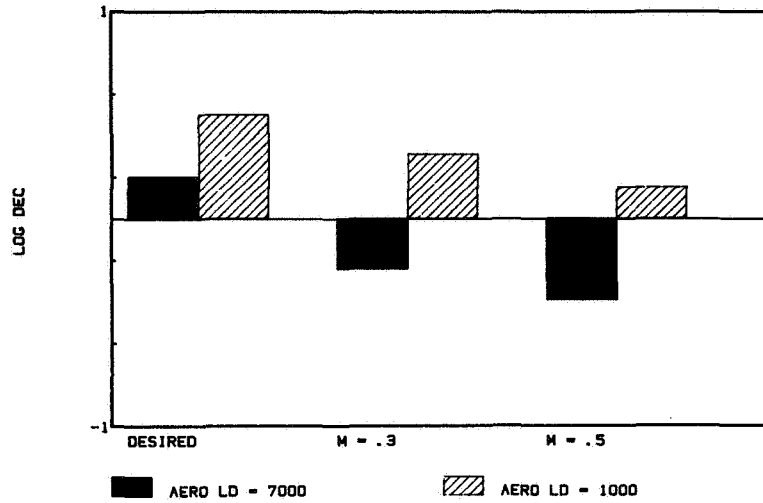


Figure 11. - Predicted stability as a function of preload for original rotor in mod 1 bearings. Speed, 12 000 rpm.

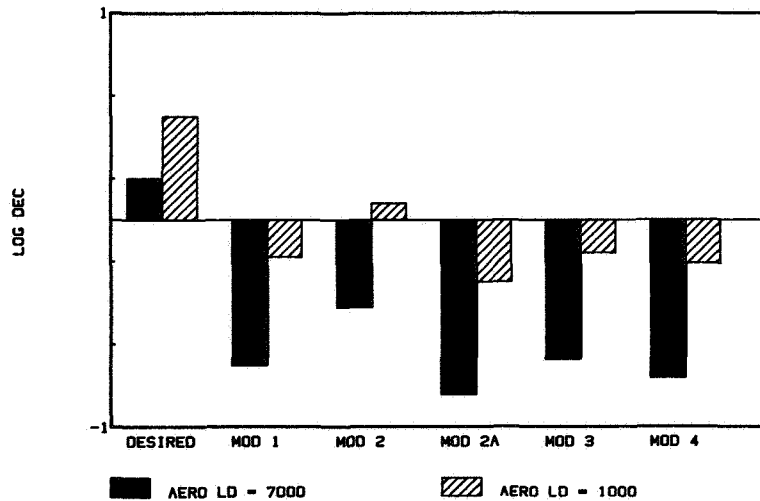


Figure 12. - Predicted log decrement as a function of various bearing modifications for original rotor. Speed, 12 000 rpm.

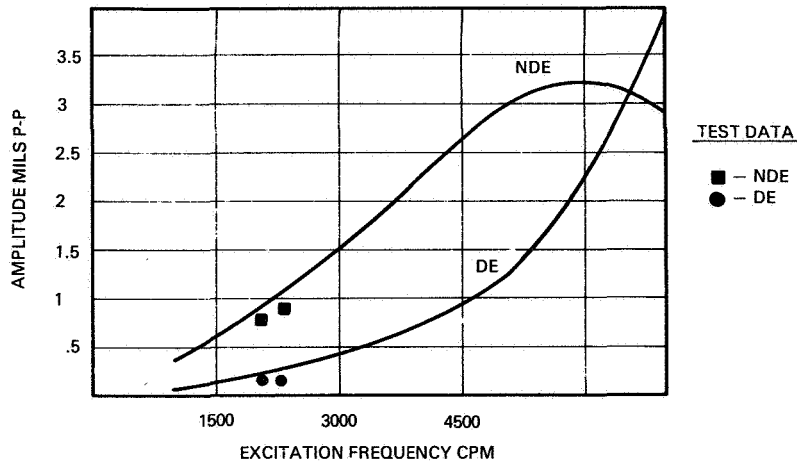


Figure 13. - Predicted response to rotating force applied near last stage at 21 percent speed - comparison of predictions with test data for original rotor in mod 1 bearings.

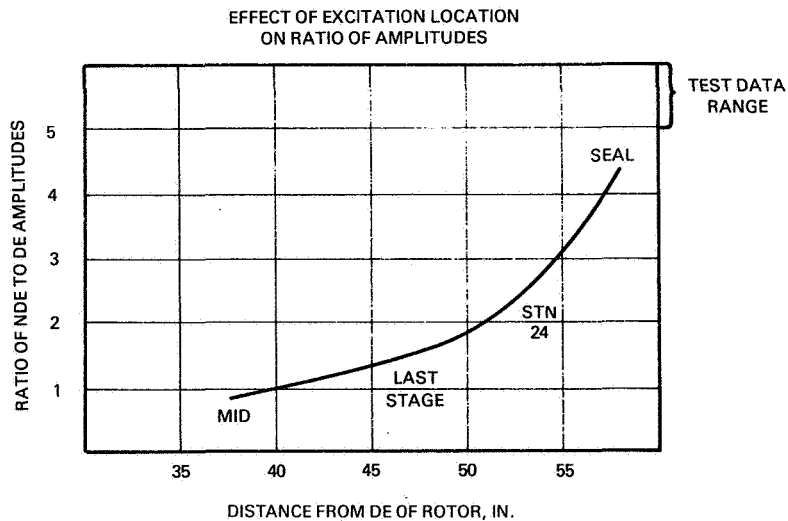


Figure 14. - Ratio of amplitudes for excitation at 21 percent of running speed as a function of excitation location for original rotor in mod 1 bearings.

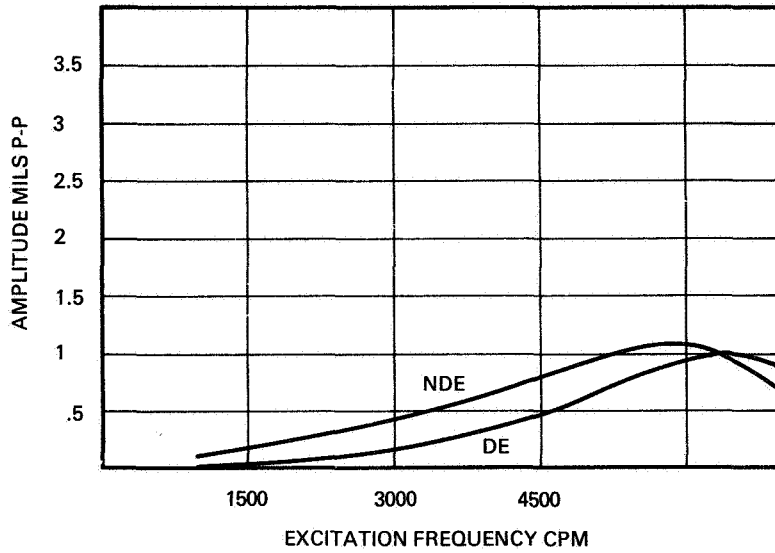


Figure 15. - Predicted response to rotating force excitation at last stage for original rotor in original bearings. Frequency of excitation, 21 percent of running speed.

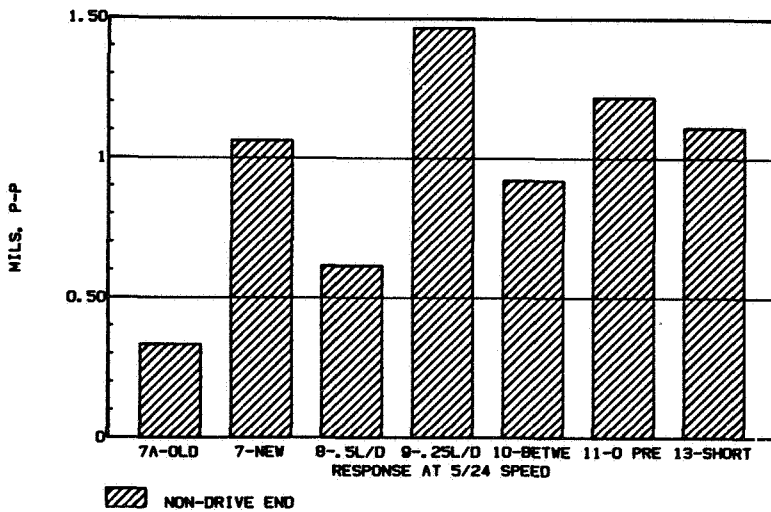


Figure 16. - Response at 21 percent of running speed as a function of bearing parameter changes.

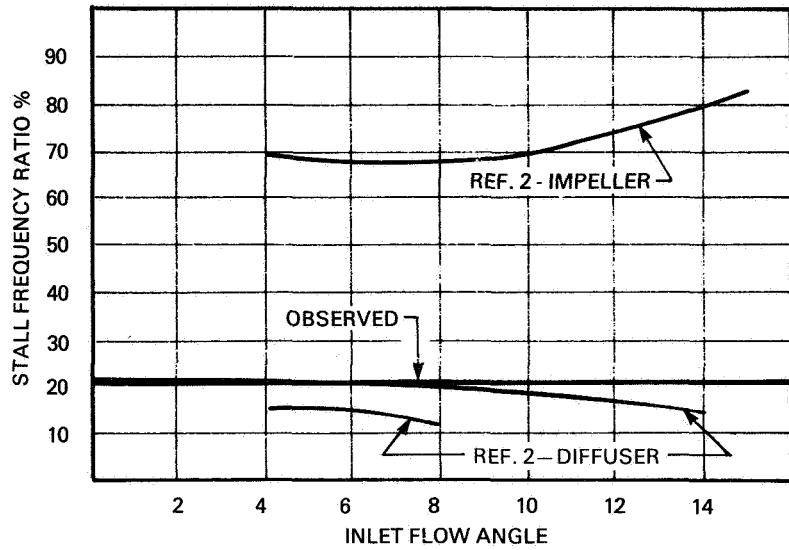


Figure 17. - Comparison of observed vibration frequency with data of reference 2.

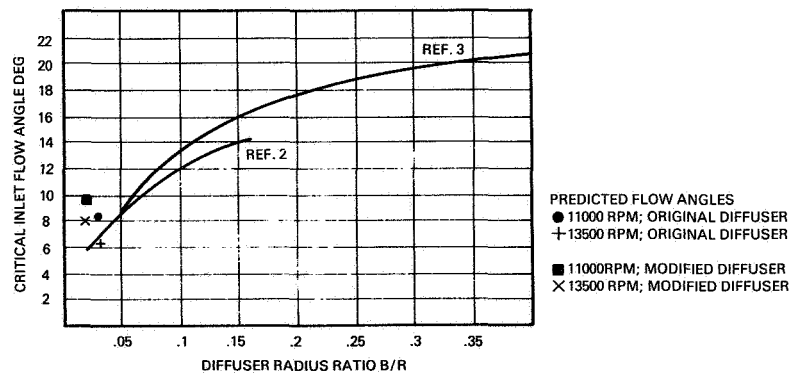


Figure 18. - Comparison of published data for diffuser rotating stall criteria.

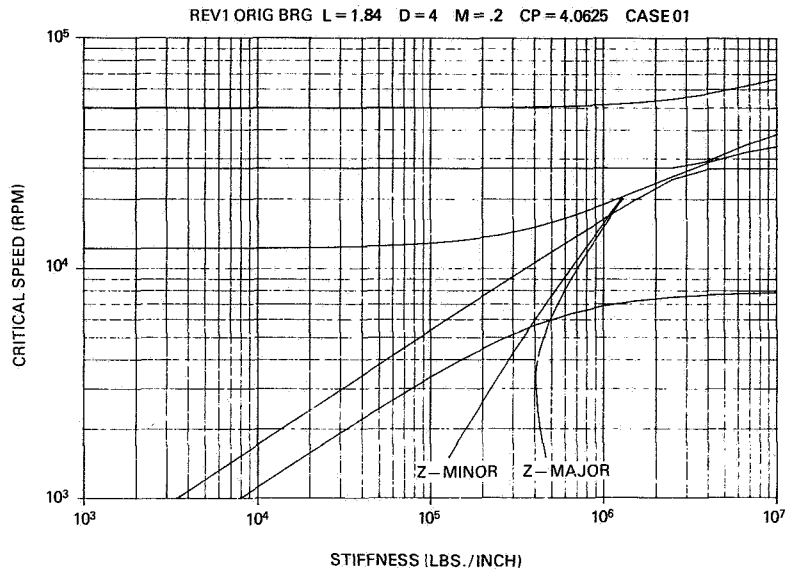


Figure 19. - Critical speed map for revised rotor.

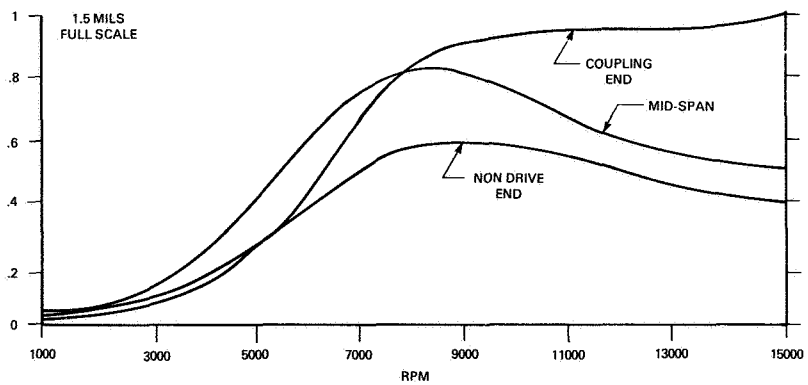


Figure 20. - Unbalanced response prediction for revised rotor in revised bearings with 1 in-oz at midspan.

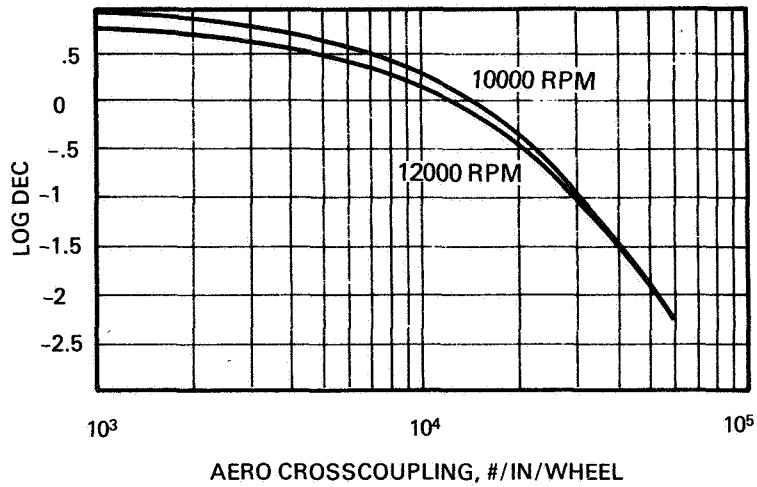


Figure 21. - Rotor stability analysis for revised rotor in revised bearings.

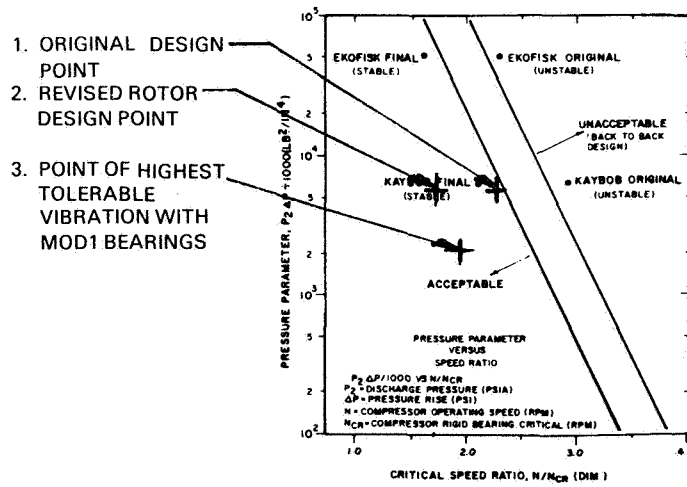


Figure 22. - Comparison of data from present study with suggested criteria of reference 6.